

Figure S1 Effect of DATS on cell viability. (A) Cell viability of B16BL6 cells treated with different concentrations of DATS (n=6). All values are mean \pm S.D. ** p <0.01 vs. 0 μ M group; *** p <0.001 vs. 0 μ M group; **** p <0.0001 vs. 0 μ M group.

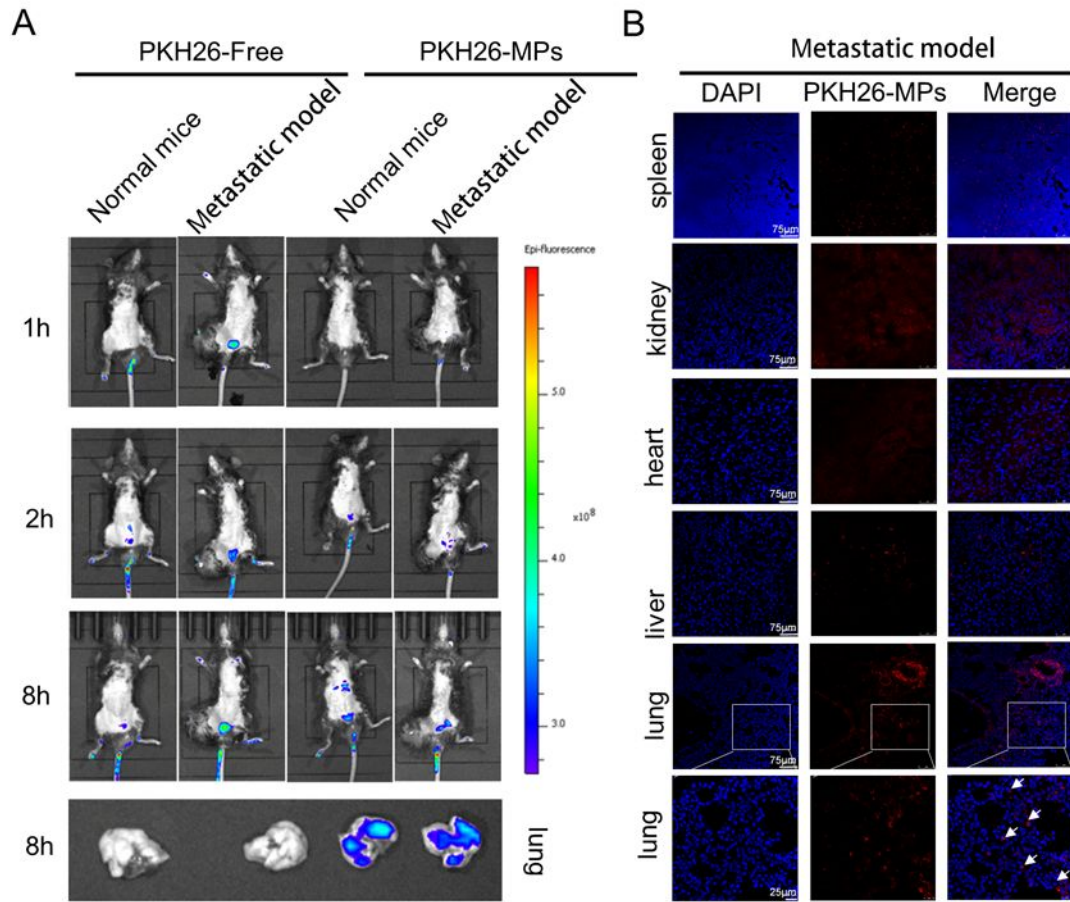


Figure S2 Biodistribution of PKH26-labelled DATS-MPs in normal (blank) and spontaneous metastatic model mice at predetermined time intervals. (A) In vivo near-infrared fluorescent images of mice after tail vein administration of PKH-26 and PKH26-MPs at different time points after administration. (B) Lung, spleen, heart, kidney and liver tissues of T-PKH26-MPs group mice were separated after 12 h, and stained with Hoechst (blue fluorescent) and observed under a laser confocal microscopy. The bottom lung tissue was the enlarged picture of the upper lung tissue. The white arrow showed the PKH26-labeled MPs taken up by lung tissue.

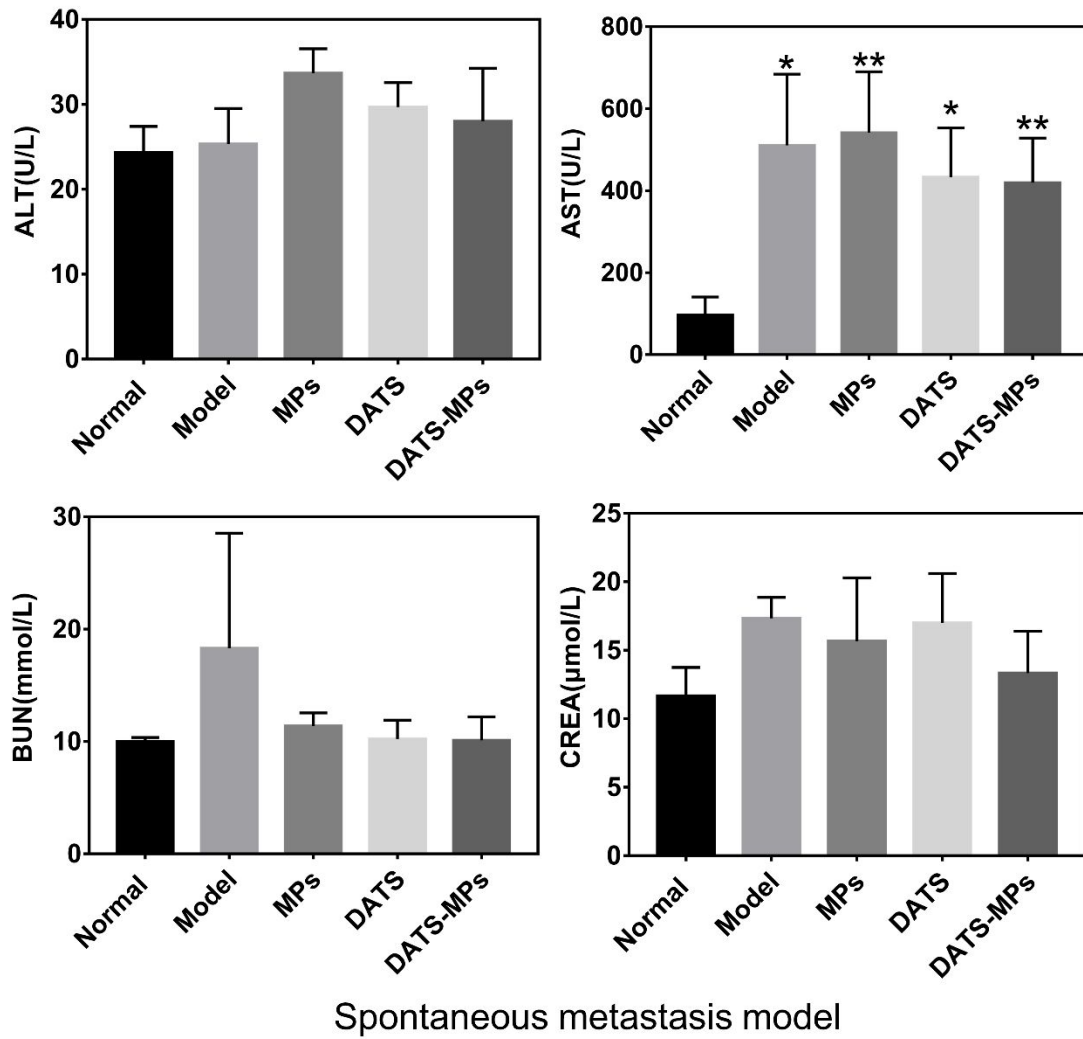
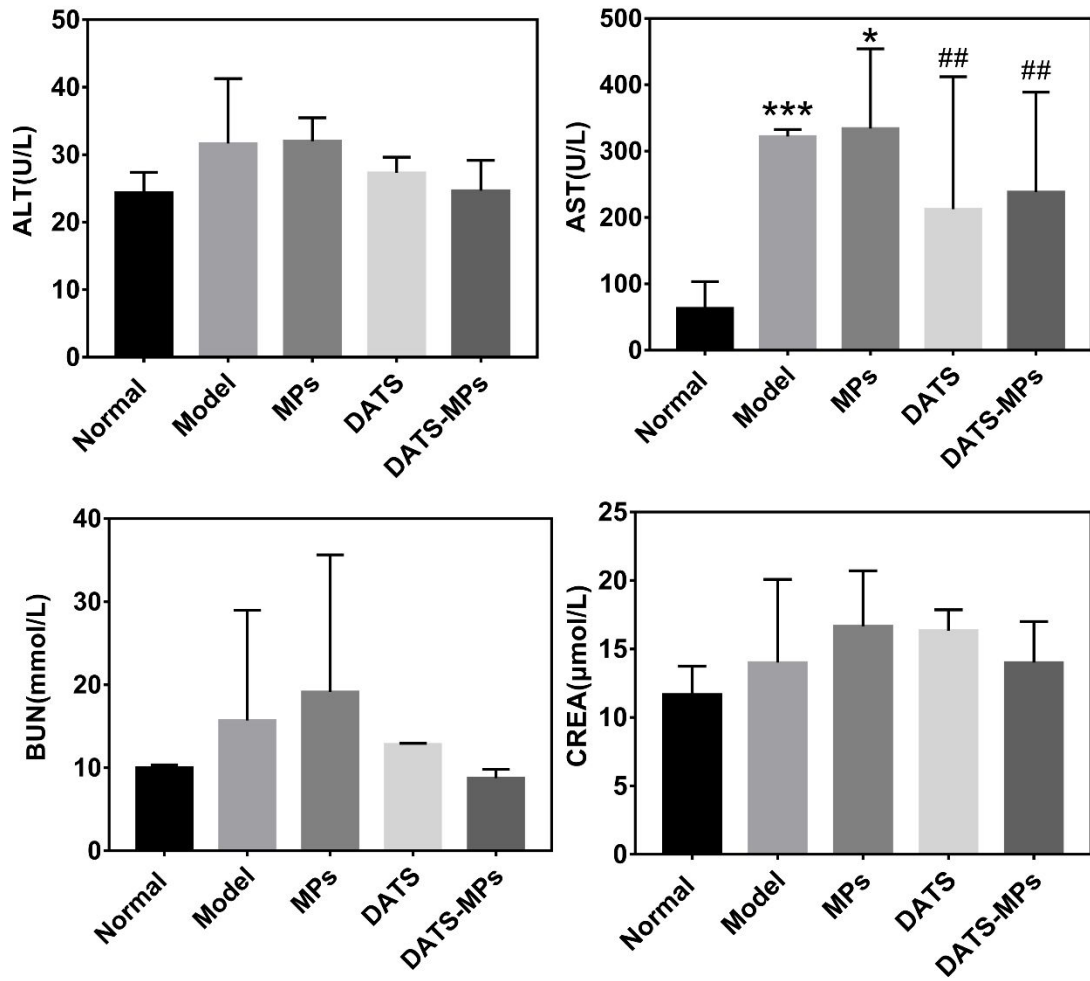


Figure S3. Safety evaluation (spontaneous model) (A and B) Comparison of liver function indices among C57BL6 spontaneous metastatic model mice after treatment. (C and D) Comparison of kidney function indices among C57BL6 spontaneous metastatic model mice after treatment. Data represent as mean \pm SD. * $p < 0.05$ vs. Blank; ** $p < 0.01$ vs. Blank.



Experimental metastasis model

Figure S4. Safety evaluation (experimental model) (A and B) Comparison of liver function indices among C57BL6 experimental metastatic model mice after treatment. (C and D) Comparison of kidney function indices among C57BL6 spontaneous metastatic model mice after treatment. Data represent as mean \pm SD. * $p < 0.05$ vs. Blank; *** $p < 0.001$ vs. Blank; ## $p < 0.01$ vs. Model.